Tracer Advection I

Atmospheric tracer transport & design philosophies

Peter Hjort Lauritzen

Atmospheric Modeling and Predictability Section (AMP)
Climate and Global Dynamics Division (CGD)
NCAR Earth System Laboratory (NESL)
National Center for Atmospheric Research (NCAR)

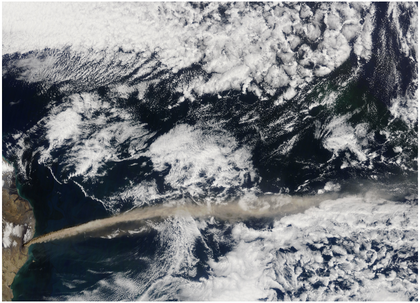

DCMIP Summer School

Picture: Eruption of Iceland's Eyjafjallajökull volcano (NASA-MODIS)

1. Continuity equation's in climate models

2. Desirable properties for transport schemes intended for climate applications
   - Mass-conservation, shape-preservation, multi-tracer efficiency, ...
   - Preservation of pre-existing functional relations (correlations) between species

3. A semi-Lagrangian view on finite-volume schemes

Continuity equation for dry air mass

$$\frac{\partial \rho}{\partial t} + \nabla \cdot (\rho \vec{v}) = 0,$$

where $\vec{v}$ is the velocity field and ρ density.

- Mass of dry air $\approx N_2$ (ca. 78.08%), O_2 (ca. 20.95%), Ar (ca. 0.93%), CO_2 (at present ca. 0.038%); these well-mixed gases make up 99.998% of the volume of dry air
- Trenberth and Smith (2005) estimated that the mass of dry air corresponds to a surface pressure of 983.05 hPa and it varies less than 0.01 hPa based on changes in atmospheric composition.
- $\Rightarrow$ to a very good approximation there are no source/sink terms on the right-hand side of continuity equation for dry air.

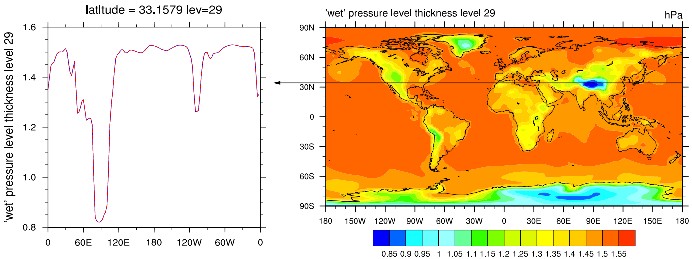

Continuity equations in climate models: water

Continuity equations for water species

$$\frac{\partial\left(\rho q_i\right)}{\partial t}+\nabla\cdot\left(\rho q_i \vec{v}\right)=P_{\rho\, q_i},$$

where q_i are dry mixing ratios[a] $[m_i^{(d)}/m^{(d)}]$ and P represent source and sink terms.

- q_i: water vapor, cloud liquid and cloud ice.
  - 99% of the total weight of the atmosphere is the mass of dry air. The remanding 1% is approximately the mass of water (large local variations though!)
- q_i: Meso-scale models also have prognostic rain, snow, graupel, ...
  - If rain, snow, graupel, etc. are diagnostic it is assumed that they fall to the ground in one physics time-step!

[a] the subtleties between using 'dry' and 'wet' mixing ratios is not discussed here - see, e.g., Lauritzen et al. (2011b)

Continuity equations in climate models: water

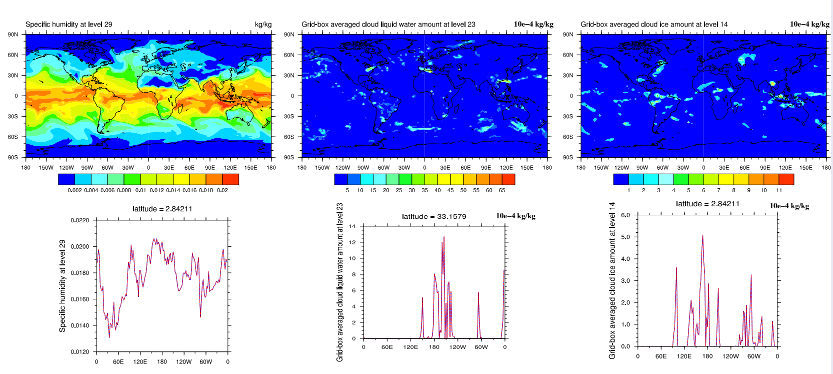

Very 'oscillatory' fields:

- Production/loss terms are large, however, clouds (e.g., 'ice clouds' such as Cirrus) can have lifetimes on the order of days
- Transport operator must not produce negative values.
- Overshooting in water vapor, for example, can trigger irreversible physical processes.

In other words: the transport scheme should be **shape-preserving** with respect to q.

- Microphysics: continuity equations for aerosol number and mass concentrations
  - CAM5 physics: 22 aerosol continuity equations (particulate organic matter, dust, sea salt, secondary organic aerosols, ...)

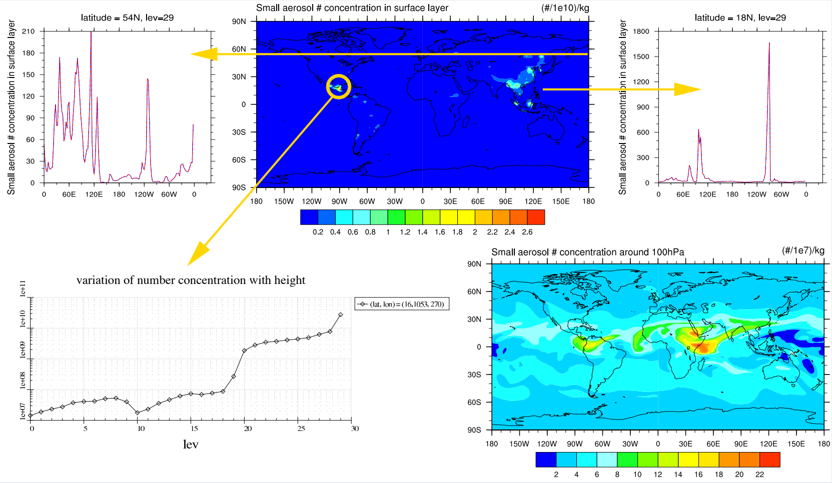

- Chemistry: continuity equations for chemical species
  - CAM-chem: approximately 127 continuity equations (ozone, chlorine compounds, bromine, ...) ... some highly reactive and some long-lived

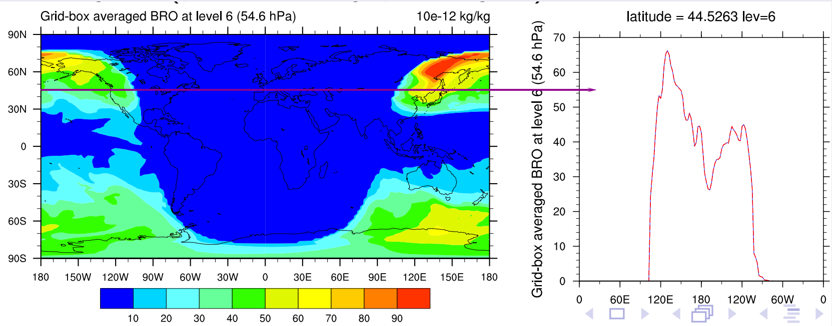

Figure: Bromine has a strong diurnal cycle (produced by photolysis)

Continuity equations in climate models: desirable properties

Important properties of transport schemes intended for atmospheric models:

- The number of prognostic continuity equations in climate and chemistry-climate models is increasing fast to accommodate more advanced physical parameterizations (e.g., microphysics), online chemistry, ...

  $\Rightarrow$ multi-tracer efficiency is becoming increasingly important
  (closely tied to compute platform)!

- Atmospheric tracer fields can have very large gradients:
  - Shape-preservation is paramount!
  - Preservation of gradients is important
- Inherent conservation of mass is desirable, in particular, to consistently enforce shape-preservation and tracer-air mass consistency.
- Optimal preservation of pre-existing functional relationships (correlations)

Correlations between longlived species in the stratosphere

Relationships between long-lived stratospheric tracers, manifested in similar spatial structures on scales ranging from a few to several thousand kilometers, are displayed most strikingly if the mixing ratio of one is plotted against another, when the data collapse onto remarkably compact curves. - Plumb (2007)

E.g., nitrous oxide (N_2O) against 'total odd nitrogen' (NO_y) or chlorofluorocarbon (CFC's)

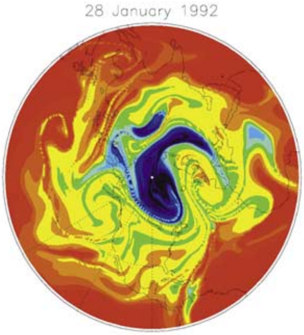

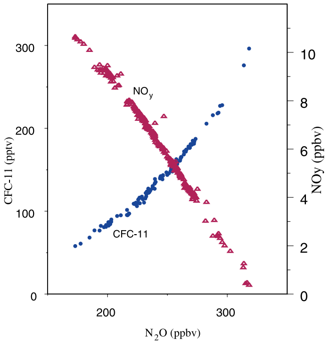

Figures from Plumb (2007).

Correlations between longlived species in the stratosphere

Relationships between long-lived stratospheric tracers, manifested in similar spatial structures on scales ranging from a few to several thousand kilometers, are displayed most strikingly if the mixing ratio of one is plotted against another, when the data collapse onto remarkably compact curves. - Plumb (2007)

E.g., nitrous oxide (N_2O) against 'total odd nitrogen' (NO_y) or chlorofluorocarbon (CFC's)

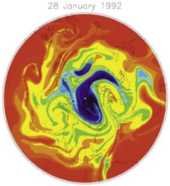

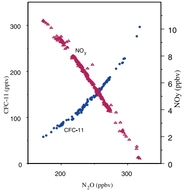

Similarly:

- The total of chemical species within some chemical family may be preserved following an air parcel although the individual species have a complicated relation to each other and may be transformed into each other through chemical reactions (e.g., total chlorine)
- Aerosol-cloud interactions (Ovtchinnikov and Easter, 2009)

The transport operator should ideally not perturb pre-existing functional relationships

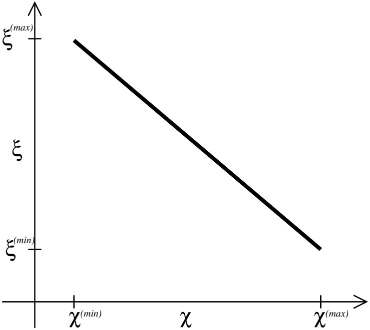

Analytical pre-existing functional relationship curve ψ (linear)

$$\xi = \psi(\chi) = a \cdot \chi + b, \quad \chi \in \left[\chi^{(min)}, \chi^{(max)}\right],$$

where a and b are constants, and χ and ξ are the mixing ratios of the two tracers

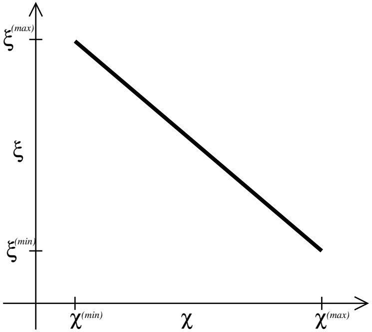

Analytical pre-existing functional relationship curve ψ (linear)

χ and ξ are transported separately by the transport scheme

$$\begin{aligned} \chi_k^{n+1} &= \mathcal{T}(\chi_j^n), \qquad j \in \mathcal{H}, \\ \xi_k^{n+1} &= \mathcal{T}(\xi_j^n), \qquad j \in \mathcal{H}, \end{aligned}$$

where $\mathcal{T}$ is the transport operator and $\mathcal{H}$ the set of indices defining the 'halo' for $\mathcal{T}$.

Analyzing scatter plots

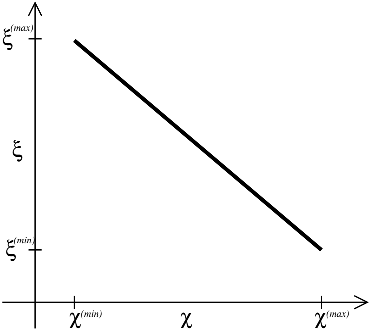

Analytical pre-existing functional relationship curve ψ (linear)

If $\mathcal{T}$ is 'semi-linear' then linear pre-existing functional relations are preserved:

$$\xi_k^{n+1} = \mathcal{T}(\xi_j^n) = \mathcal{T}(a\,\chi_j^n + b) = a\mathcal{T}(\chi_j^n) + b\mathcal{T}(1) = a\mathcal{T}(\chi_j^n) + b = a\chi_k^{n+1} + b.$$

$\rightarrow$ If transport operator is non-linear the relationship might be violated.

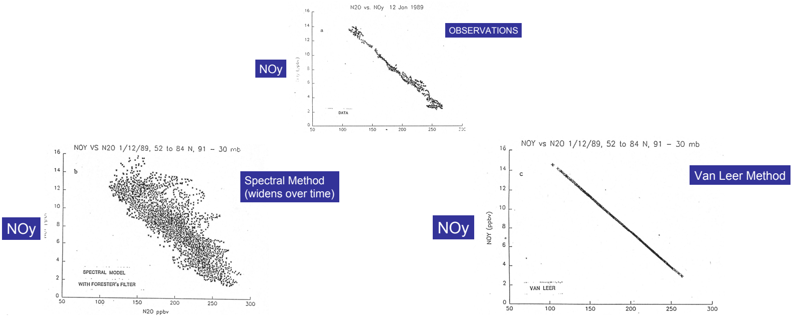

Figures from R.Rood's talk at the 2008 NCAR ASP colloquium

Analytical pre-existing functional relationship curve ψ (linear)

$\rightarrow$ carefully designed finite-volume schemes are 'semi-linear' even with limiters/filters! (Thuburn and McIntyre, 1997; Lin and Rood, 1996)

Analyzing scatter plots

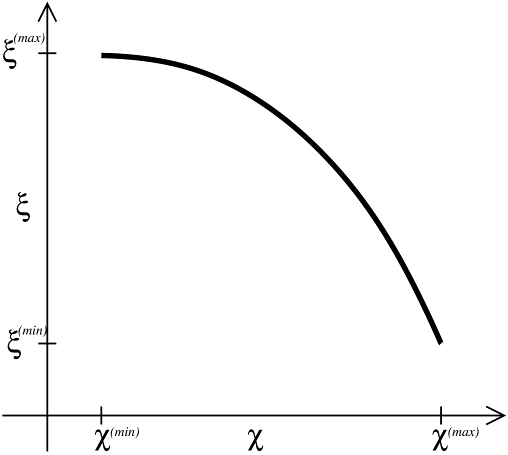

Analytical pre-existing functional relationship curve ψ

$$\xi = \psi(\chi) = a \cdot \chi^2 + b,$$

where a and b are constants so that ψ is concave or convex in $\left[\chi^{(min)}, \chi^{(max)}\right]$

Analyzing scatter plots

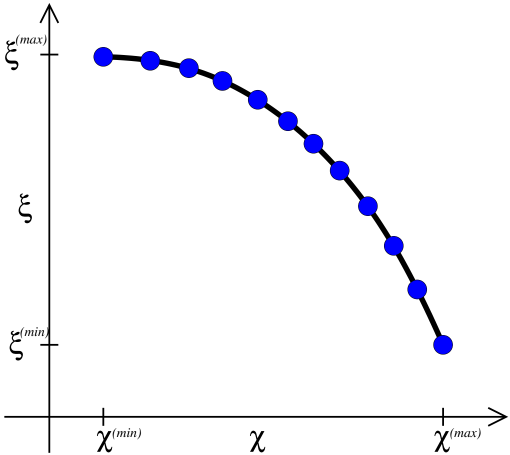

Discrete pre-existing functional relation (initial condition)

$$\xi_k = \psi(\chi_k) = a \cdot (\chi_k)^2 + b, \quad k = 1, .., K,$$

where a and b are constants so that ψ is concave or convex in $\left[\chi^{(min)}, \chi^{(max)}\right]$

Analyzing scatter plots

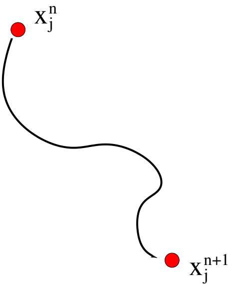

A fully Lagrangian model will maintain pre-existing functional relation

$$\chi_k^{n+1} = \chi_k^n, \qquad \xi_k^{n+1} = \xi_k^n$$

following parcel trajectories (without 'contour-surgery' or other mixing mechanisms)

Analyzing scatter plots

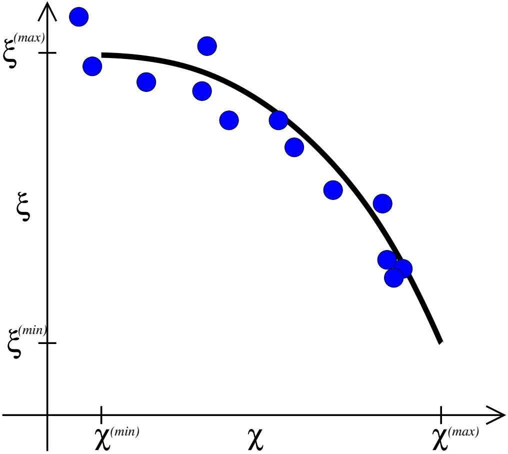

Any Eulerian/semi-Lagrangian scheme will disrupt pre-existing functional relation

$$\xi_k^{n+1} = \mathcal{T}(\xi_j^n) \neq a \cdot \mathcal{T}\left(\chi_j^n\right)^2 + b, \quad j \in \mathcal{H}$$

where $\mathcal{T}$ is the transport operator and $\mathcal{H}$ the set of indices defining the 'halo' for $\mathcal{T}$.

‘Real’ mixing, e.g., observed during polar vortex breakup (Waugh et al., 1997)

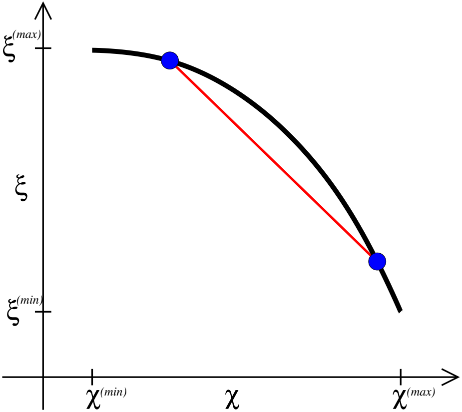

‘Real mixing’ (when occurring) will tend to replace the functional relation by a scatter by linearly interpolating along mixing lines between pairs of points

'Real' mixing, e.g., observed during polar vortex breakup (Waugh et al., 1997)

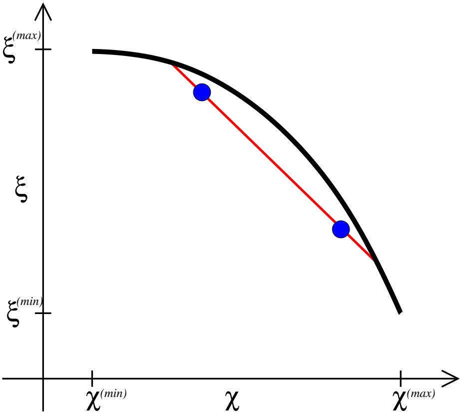

'Real mixing' (when occurring) will tend to replace the functional relation by a scatter by linearly interpolating along mixing lines between pairs of points
$\rightarrow$ Ideally numerical mixing should = 'real mixing'!

However, it may be shown mathematically that schemes that exclusively introduce 'real mixing' are 1^{st}-order schemes (Thuburn and McIntyre, 1997).

Classification of numerical mixing on scatter plots

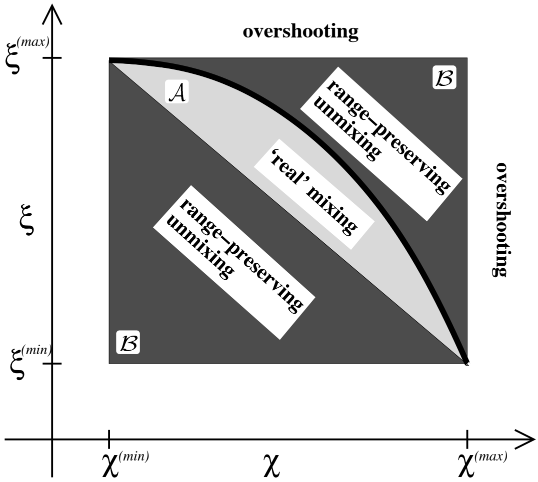

Figure from (Lauritzen and Thuburn, 2012)

Show animation from idealized test case (Lauritzen and Thuburn, 2012; Lauritzen et al., 2012)

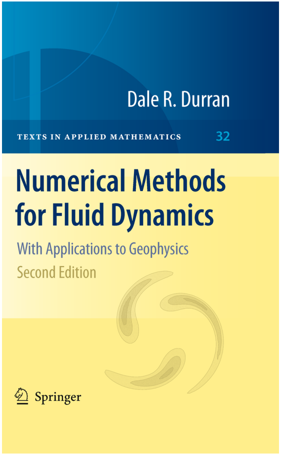
Dale R. Durran
TEXTS IN APPLIED MATHEMATICS
32
Numerical Methods for Fluid Dynamics
With Applications to Geophysics
Second Edition
Springer

Derivation form

'Most fundamental equations in fluid dynamics can derived from first principles in either a *Eulerian* form or an *Lagrangian* form' - (see, e.g., text book of Durran, 1999)

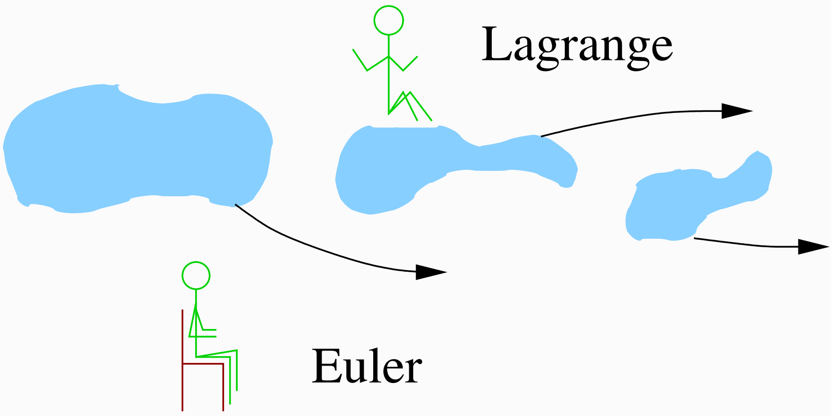

Figure courtesy of J. Thuburn.

Consider the continuity equation for some inert (no sources/sinks) and passive (does not feed back on the flow) tracer

semi-Lagrangian form

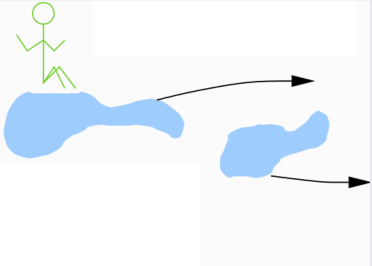

Eulerian (flux) form

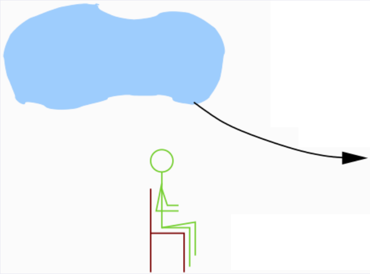

For simplicity assume a quadrilateral mesh and leave out the ‘details’ of spherical geometry.

- Only consider two-time-level finite-volume schemes

Finite-volume approach: Integrate in space

semi-Lagrangian form

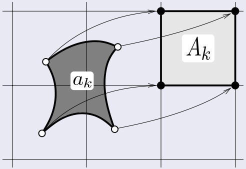

$$\frac{D}{Dt}\int_{A(t)} \psi \, dA = 0.$$

where $A(t)$ is a Lagrangian† control volume and

$$\frac{D}{Dt} = \frac{\partial}{\partial t} + \vec{v}\cdot\nabla,$$

is the material/total derivative.

Eulerian (flux-form) form

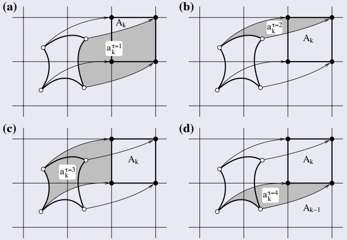

Integrate

$$\frac{\partial \psi}{\partial t} + \nabla\cdot(\psi\,\vec{v}) = 0$$

over an Eulerian control volume A_k:

$$\frac{\partial}{\partial t}\int_{A_k} \psi \, dA + \int_{A_k} \nabla\cdot(\psi\,\vec{v}) \, dA = 0.$$

† volume whose bounding surface moves with the local fluid velocity $\Leftrightarrow$ volume which always contains the same material particles

semi-Lagrangian form

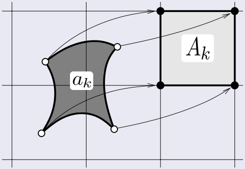

$$\frac{D}{Dt}\int_{A(t)} \psi \, dA = 0.$$

where $A(t)$ is a Lagrangian† control volume and

$$\frac{D}{Dt} = \frac{\partial}{\partial t} + \vec{v}\cdot\nabla,$$

is the material/total derivative.

Eulerian (flux-form) form

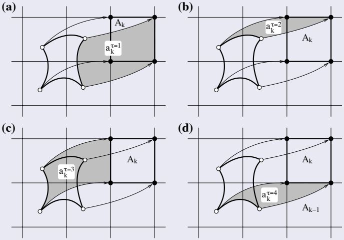

Apply divergence theorem on second term:

$$\frac{\partial}{\partial t}\int_{A_k} \psi \, dA + \oint_{\partial A_k} (\psi\,\vec{v})\cdot\vec{n}\,dS = 0,$$

where ∂A_k is the boundary of A_k and $\vec{n}$ the outward normal vector to ∂A_k.
$\rightarrow$ instantaneous flux of tracer mass through boundaries of A_k

†volume whose bounding surface moves with the local fluid velocity $\Leftrightarrow$ volume which always contains the same material particles

Finite-volume approach: Integrate in time

semi-Lagrangian form

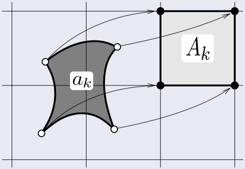

$$\int_{A(t+\Delta t)} \psi \, dA = \int_{A(t)} \psi \, dA,$$

where Δt is time-step and $t = n\,\Delta t$.

Upstream semi-Lagrangian approach:

$$\overline{\psi}_k^{n+1} \Delta A_k = \overline{\psi}_k^{n} \Delta a_k,$$

where $\overline{()}$ is average value over cell.

Eulerian (flux-form) form

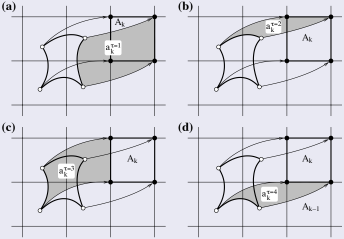

Apply divergence theorem on second term:

$$\frac{\partial}{\partial t} \int_{A_k} \psi \, dA + \oint_{\partial A_k} (\psi \, \vec{v}) \cdot \vec{n} \, dS = 0,$$

where ∂A_k is the boundary of A_k and $\vec{n}$ the outward normal vector to ∂A_k.
$\rightarrow$ instantaneous flux of tracer mass through boundaries of A_k

semi-Lagrangian form

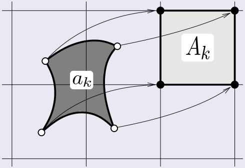

$$\int_{A(t+\Delta t)} \psi \, dA = \int_{A(t)} \psi \, dA,$$

where Δt is time-step and $t = n\,\Delta t$.

Upstream semi-Lagrangian approach:

$$\overline{\psi}_k^{n+1} \Delta A_k = \overline{\psi}_k^{n} \Delta a_k,$$

where $\overline{()}$ is average value over cell.

Eulerian (flux-form) form

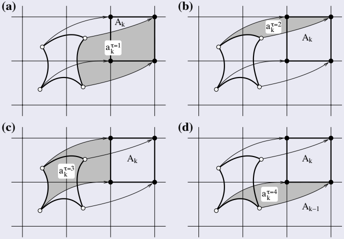

$$\frac{\partial}{\partial t}\int_{A_k} \psi \, dA + \oint_{\partial A_k} (\psi\,\vec{v}) \cdot \vec{n}\, dS = 0,$$

$$\overline{\psi}^{n+1} \Delta A_k = \overline{\psi}^{n} \Delta A_k +$$

$$\int_{n\Delta t}^{(n+1)\Delta t} \left[\oint_{\partial A_k} (\psi\,\vec{v}) \cdot \vec{n}\, dS \right] dt = 0,$$

$\rightarrow$ flux of tracer mass through boundaries of A_k during $t \in [n\Delta t, (n+1)\Delta t]$

Finite-volume approach:

semi-Lagrangian form

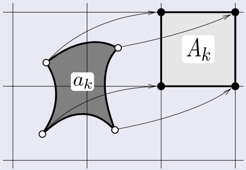

$$\int_{A(t+\Delta t)} \psi \, dA = \int_{A(t)} \psi \, dA,$$

where Δt is time-step and $t = n\,\Delta t$.

Upstream semi-Lagrangian approach:

$$\overline{\psi}_k^{n+1} \Delta A_k = \overline{\psi}_k^{n} \Delta a_k,$$

where $\overline{()}$ is average value over cell.

Eulerian (flux-form) form

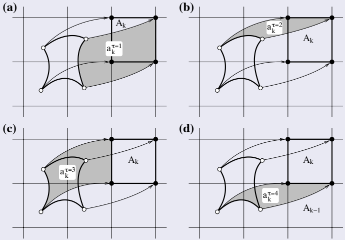

$$\overline{\psi}_k^{n+1} \Delta A_k = \overline{\psi}_k^{n} \Delta A_k - \sum_{\tau=1}^{4} F_k^{(\tau)},$$

where

$$F_k^{(\tau)} = s_k^{(\tau)} \int_{a_k^{\tau}} \psi^n(x,y)\, dA.$$

is flux of mass through face τ during Δt, and $s_k^{(\tau)} = \pm 1$

for simplicity assume s_k^{τ} is NOT multi-valued; for multi-valued case see, e.g., Harris et al. (2010).

semi-Lagrangian form

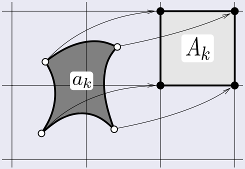

$$\overline{\psi}_k^{n+1}\Delta A_k = \overline{\psi}_k^{n}\Delta a_k,$$

Eulerian (flux-form) form

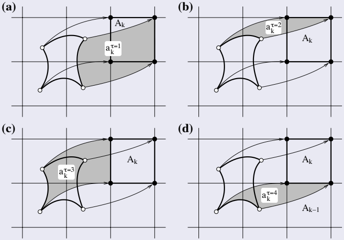

$$\overline{\psi}_k^{n+1}\,\Delta A_k = \overline{\psi}_k^{n}\,\Delta A_k - \sum_{\tau=1}^{4} F_k^{(\tau)},$$

Note equivalence between Lagrangian cell-integrated and Eulerian flux-form continuity equations:

$$\Delta A_k - \sum_{\tau=1}^{4}\left(s_k^{(\tau)}\,\Delta a_k^{(\tau)}\right) = \Delta a_k.$$

i.e. the areas involved in Eulerian forecast equals upstream Lagrangian area a_k.

semi-Lagrangian form

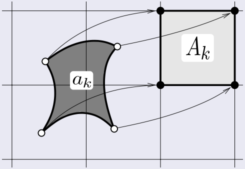

$$\overline{\psi}_k^{n+1}\Delta A_k = \overline{\psi}_k^{n}\Delta a_k,$$

Define a global piecewise continuous reconstruction function

$$\psi(x,y) = \sum_{k=1}^{N} I_{A_k}\psi_k(x,y),$$

where I_{A_k} is the indicator function

$$I_{A_k} = \begin{cases} 1, \ (x,y) \in A_k, \\ 0, \ (x,y) \notin A_k. \end{cases}$$

Eulerian (flux-form) form

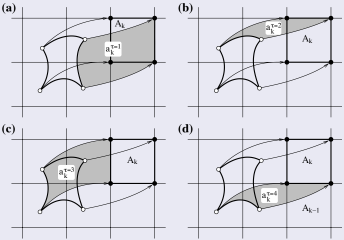

$$\overline{\psi}_k^{n+1}\,\Delta A_k = \overline{\psi}_k^{n}\,\Delta A_k - \sum_{\tau=1}^{4} F_k^{(\tau)},$$

semi-Lagrangian form

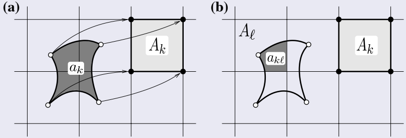

$$\overline{\psi}_k^{n+1}\Delta A_k = \overline{\psi}_k^{n}\Delta a_k,$$

$$\overline{\psi}_k^{n+1}\,\Delta A_k = \sum_{\ell=1}^{L_k}\int_{a_{k\ell}} \psi_\ell^n(x,y)\,dA.$$

where $a_{k\ell}$ is the non-empty overlap area

$$a_{k\ell} = a_k \cap A_\ell, \quad a_{k\ell} \neq \emptyset; \quad \ell = 1,\ldots,L_k,$$

where N is the number of cells in the domain and L_k number of overlap areas.

Eulerian (flux-form) form

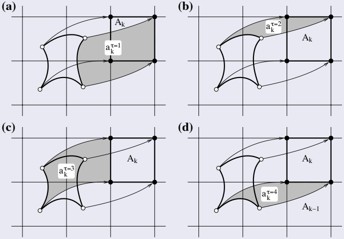

$$\overline{\psi}_k^{n+1}\,\Delta A_k = \overline{\psi}_k^{n}\,\Delta A_k - \sum_{\tau=1}^{4} F_k^{(\tau)},$$

Finite-volume approach:

semi-Lagrangian form

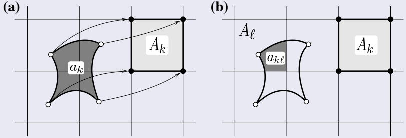

$$\overline{\psi}_k^{n+1} \Delta A_k = \overline{\psi}_k^{n} \Delta a_k,$$

$$\overline{\psi}_k^{n+1} \, \Delta A_k = \sum_{\ell=1}^{L_k} \int_{a_{k\ell}} \psi_\ell^n(x,y) \, dA.$$

where $a_{k\ell}$ is the non-empty overlap area

$$a_{k\ell} = a_k \cap A_\ell, \quad a_{k\ell} \neq \emptyset; \quad \ell = 1, \ldots, L_k,$$

where N is the number of cells in the domain and L_k number of overlap areas.

Eulerian (flux-form) form

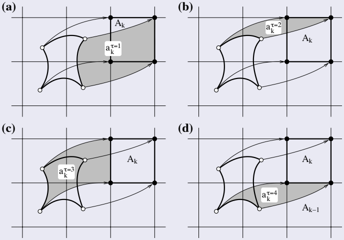

$$\overline{\psi}_k^{n+1} \, \Delta A_k = \overline{\psi}_k^{n} \, \Delta A_k - \sum_{\tau=1}^{4} F_k^{(\tau)},$$

$$F_k^{(\tau)} = \sum_{\ell=1}^{L_k^{(\tau)}} \int_{a_{k\ell}} \psi_\ell^n(x,y) \, dA,$$

where L_k^τ is number of non-empty 'flux' overlap areas for face τ.

Note that in general: $L_k \ll \sum_{\tau=1}^{4} L_k^{(\tau)}$

semi-Lagrangian form

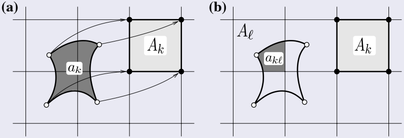

$$\overline{\psi}_k^{n+1} \Delta A_k = \overline{\psi}_k^n \Delta a_k,$$

- a_k's span Ω without gaps/overlaps

$$\bigcup_{k=1}^{N} a_k = \Omega, \text{ and } a_k \cap a_\ell = \emptyset \, \forall \, k \neq \ell.$$

- Sub-grid-scale representation of ψ must integrate to cell-average mass

$$\int_{A_k} \psi_k^n(x,y)\, dA = \overline{\psi}_k^n \Delta A,$$

Eulerian (flux-form) form

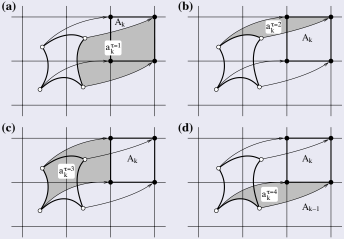

$$\overline{\psi}_k^{n+1} \Delta A_k = \overline{\psi}_k^n \Delta A_k - \sum_{\tau=1}^{4} F_k^{(\tau)},$$

- Fluxes for 'shared' faces must cancel, e.g.,

$$F_k^{(3)} = -F_{k-1}^{(1)}$$

Any flux, even highly inaccurate fluxes, will NOT violate mass-conservation!

Finite-volume approach: Enforcing shape-preservation

semi-Lagrangian form

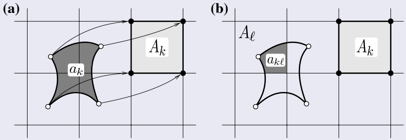

$$\overline{\psi}_k^{n+1}\Delta A_k = \overline{\psi}_k^{n}\Delta a_k,$$

The *only* direct way of enforcing shape-preservation is to filter the sub-grid-scale distribution $\psi_k^n(x,y)$:

- fully 2D filters (Barth and Jespersen, 1989)
- 1D filters for cascade schemes (Colella and Woodward, 1984; Zerroukat et al., 2005; Lin and Rood, 1996)

Eulerian (flux-form) form

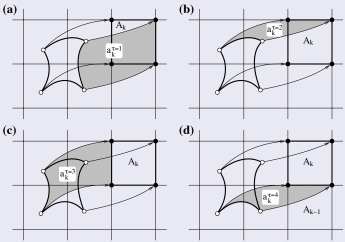

$$\overline{\psi}_k^{n+1}\Delta A_k = \overline{\psi}_k^{n}\Delta A_k - \sum_{\tau=1}^{4} F_k^{(\tau)},$$

Shape-preservation can be enforced by

- blending monotone and high-order fluxes (e.g., Flux-Corrected Transport Zalesak, 1979)
- making $\psi_k^n(x,y)$ shape-preserving (Barth and Jespersen, 1989)

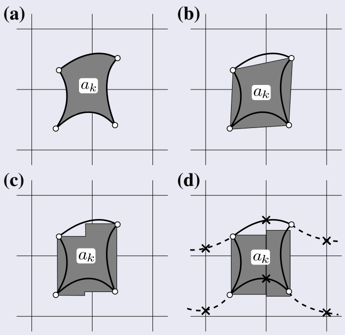

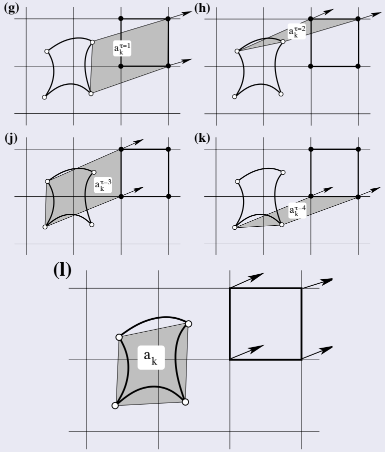

(a) Exact

(b) Straight lines (Rančić, 1992; Lauritzen et al., 2010)

(c) Step-functions for ‘North/South’ faces & straight lines parallel to ‘longitudes’ for ‘East/West’ faces (Nair and Machenhauer, 2002).

(d) Cascade (flow-split) (Nair et al., 2002; Zerroukat et al., 2002)

(g-k) Quadrilateral flux-areas (Dukowicz and Baumgardner, 2000; Harris et al., 2010)

(l) ‘Effective’ departure area

Finite-volume approach: Area approximation

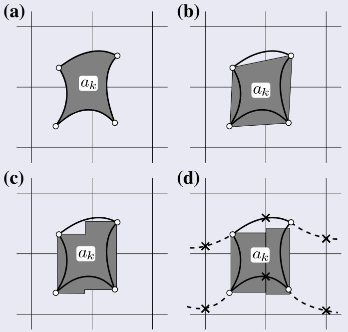

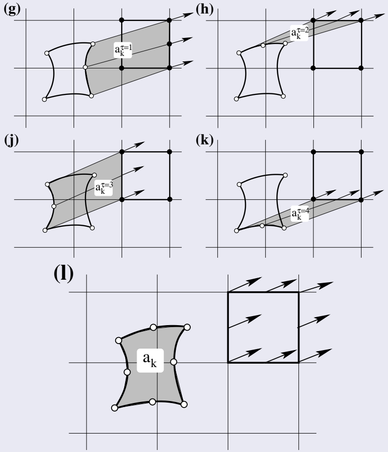

(a) Exact

(b) Straight lines (Rančić, 1992; Lauritzen et al., 2010)

(c) Step-functions for ‘North/South’ faces & straight lines parallel to ‘longitudes’ for ‘East/West’ faces (Nair and Machenhauer, 2002).

(d) Cascade (flow-split) (Nair et al., 2002; Zerroukat et al., 2002)

(g-k) ‘Curved’ (parabolic) flux-areas (Ullrich et al., 2012)

(l) ‘Effective’ departure area

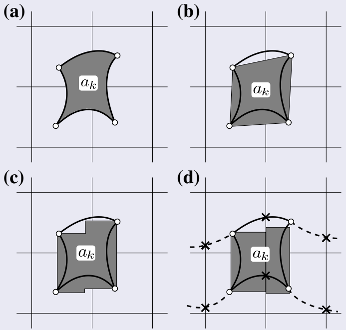

(a) Exact

(b) Straight lines (Rančić, 1992; Lauritzen et al., 2010)

(c) Step-functions for ‘North/South’ faces & straight lines parallel to ‘longitudes’ for ‘East/West’ faces (Nair and Machenhauer, 2002).

(d) Cascade (flow-split) (Nair et al., 2002; Zerroukat et al., 2002)

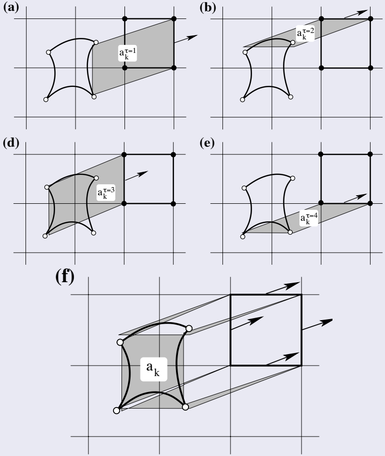

(g-k) Parallelogram flux-areas (Miura, 2007; Skamarock and Menchaca, 2010)

(l) ‘Effective’ departure area

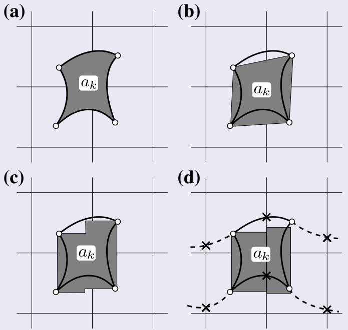

(a) Exact

(b) Straight lines (Rančić, 1992; Lauritzen et al., 2010)

(c) Step-functions for 'North/South' faces & straight lines parallel to 'longitudes' for 'East/West' faces (Nair and Machenhauer, 2002).

(d) Cascade (flow-split) (Nair et al., 2002; Zerroukat et al., 2002)

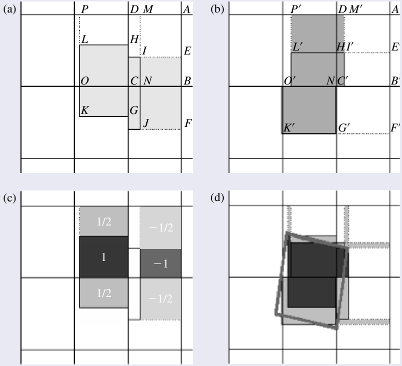

Figure from Machenhauer et al. (2009)

(a-c) Dimensionally split scheme (Lin and Rood, 1996): Flux-areas area combinations of rectangles aligned with grid lines

(d) 'Effective' departure area

Finite-volume approach: Geometric and reconstruction errors

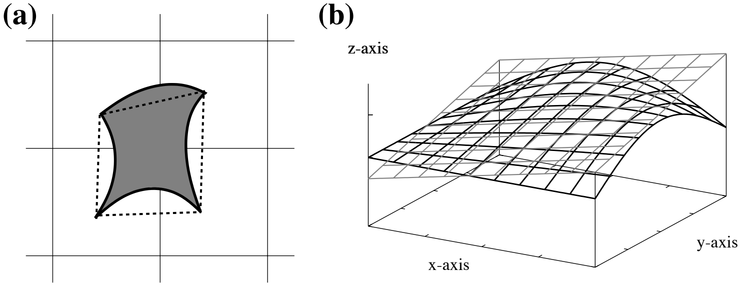

Geometric error ***Reconstruction error***

- **'geometric error'**: how well is the upstream Lagrangian area / flux areas approximated
- **'reconstruction error'**: how well is the sub-grid-scale distribution approximated
  (methods for reconstructions was discussed in P.A. Ullrich's lecture 1)

Typically:

- for lower-order reconstruction functions the 'reconstruction error' $\gg$ 'geometric error'
- the smaller the Courant number (Δt) the smaller the 'geometric error'
- for higher-order reconstruction functions and shear flows (deformational) the 'geometric error' can be significant (Ullrich et al., 2012)

Recall: we can do anything we want with the fluxes as long as $F_k^{(3)} = -F_{k-1}^{(1)}$

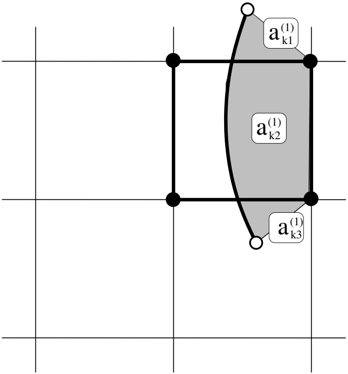

'Rigorous' flux for face 1 ($\tau = 1$):

$$F_k^{(1)} = \sum_{\ell=1}^{3} \int_{a_{k\ell}} \psi_\ell^n(x,y)\, dA.$$

For Δt sufficiently small:

$$\Delta a_{k2} \gg \Delta a_{k1} \text{ and } \Delta a_{k2} \gg \Delta a_{k3}$$

$\rightarrow$ simplify flux-integration by only using one upstream reconstruction function:

$$F_k^{(1)} \approx \mathcal{F}_k^{(1)} = \int_{a_{k1} \cup a_{k2} \cup a_{k3}} \psi_2^n(x,y)\, dA.$$

ψ_2^n is extrapolated over a_{k1} and a_{k3}.

- note: the search for overlap areas has almost been eliminated in $\mathcal{F}_k^{(1)}$
- $\mathcal{F}_k^{(1)}$ stable for Courant numbers approximately less than $\frac{1}{2}$ ($\Delta a_{k2} > \Delta a_{k1} + \Delta a_{k3}$) (Lauritzen et al., 2011a)
- $\mathcal{F}_k^{(1)}$ can be slightly more accurate than $F_k^{(1)}$ (Lauritzen et al., 2011a)

Time-stepping and coupling: stability

The η-coordinate atmospheric primitive equations, neglecting dissipation and forcing terms:

$$\frac{\partial \vec{v}}{\partial t} + (\zeta + f)\,\hat{k}\times\vec{v} + \nabla\left(\frac{1}{2}\vec{v}^2 + \Phi\right) + \dot{\eta}\frac{\partial \vec{v}}{\partial \eta} + \frac{RT_v}{p}\nabla p = 0 \quad (1)$$

$$\frac{\partial T}{\partial t} + \vec{v}\cdot\nabla T + \dot{\eta}\frac{\partial T}{\partial \eta} - \frac{RT_v}{c_p^* p}\omega = 0 \quad (2)$$

$$\frac{\partial}{\partial t}\left(\frac{\partial p}{\partial \eta}\right) + \nabla\cdot\left(\frac{\partial p}{\partial \eta}\vec{v}\right) + \frac{\partial}{\partial \eta}\left(\dot{\eta}\frac{\partial p}{\partial \eta}\right) = 0 \quad (3)$$

$$\frac{\partial}{\partial t}\left(\frac{\partial p}{\partial \eta}q\right) + \nabla\cdot\left(\frac{\partial p}{\partial \eta}q\vec{v}\right) + \frac{\partial}{\partial \eta}\left(\dot{\eta}\frac{\partial p}{\partial \eta}q\right) = 0. \quad (4)$$

- Continuity equation for air is coupled with momentum and thermodynamic equations:
  - thermodynamic variables and other prognostic variables feed back on the velocity field
  - which, in turn, feeds back on the solution to the continuity equation.
  - Hence the continuity equation for air can not be solved in isolation and one must obey the maximum allowable time-step restrictions imposed by the fastest waves in the system.
- The passive tracer transport equation can be solved in isolation given prescribed winds and air densities, and is therefore not susceptible to the time-step restrictions imposed by the fastest waves in the system.

Time-stepping and coupling: consistency

Continuity equation for air density ρ

$$\frac{\partial \rho}{\partial t} + \nabla \cdot (\rho\, \vec{v}) = 0, \tag{1}$$

and a tracer with mixing ratio q

$$\frac{\partial (\rho\, q)}{\partial t} + \nabla \cdot (\rho\, q\, \vec{v}) = 0, \tag{2}$$

- In continuous space:

  $q = 1 \Rightarrow$ continuity equation for $(\rho\, q)$ reduces to continuity equation for air (ρ)

- It is considered desirable that discretization schemes obey this relation:

  'free-stream' preserving or 'consistent' tracer transport.

- Note: 'complete consistency' is obtained if air density and tracer mass continuity equations are solved using the same numerical method, on the same discretization grid, and using the same **time-steps** (everything is 'in sync'!).

Time-stepping and coupling:

semi-Lagrangian form | Eulerian (flux-form) form

Time-stepping and coupling: mass-conservative semi-implicit approach

Traditionally: semi-Lagrangian advection of ρ is combined with semi-implicit time-stepping:

$$\overline{\rho}_k^{n+1} = \left(\overline{\rho}_k^{n+1}\right)_{exp} - \frac{\Delta t}{2}\rho_{00}\left(\nabla \cdot \vec{v}_k^{n+1} - \nabla \cdot \tilde{v}_k^{n+1}\right),$$

where

- ρ_{00} a constant reference density
- $(\cdot)_{exp}$ is the explicit prediction
- $\tilde{\vec{v}}^{n+1}$ velocity extrapolated to time-level $(n+1)$

What about tracers?

- Solving continuity equation for $(\rho\, q)$ explicitly

$$\overline{\rho\, q}_k^{n+1}\Delta A_k = \overline{\rho\, q}_k^{n}\Delta a_k$$

  is NOT 'free-stream' preserving!
- Using 'traditional' semi-implicit approach for tracers

$$\overline{\rho\, q}_k^{n+1}\Delta A_k = \overline{\rho\, q}_k^{n}\Delta a_k - \frac{\Delta t}{2}(\rho\, q)_{00}\left(\nabla \cdot \vec{v}_k^{n+1} - \nabla \cdot \tilde{\vec{v}}_k^{n+1}\right).$$

  is problematic (Lauritzen et al., 2008).

Traditionally: semi-Lagrangian advection of ρ is combined with semi-implicit time-stepping:

$$\overline{\rho}_k^{n+1} = \left(\overline{\rho}_k^{n+1}\right)_{exp} - \frac{\Delta t}{2}\left\{\nabla \cdot \left[\left(\overline{\rho}_k^{n+1}\right)_{exp} \vec{v}_k^{n+1}\right] - \nabla \cdot \left[\left(\overline{\rho}_k^{n}\right)_{exp} \tilde{\vec{v}}_k^{n+1}\right]\right\}.$$

where

- ρ_{00} a constant reference density
- $(\cdot)_{exp}$ is the explicit prediction
- $\tilde{\vec{v}}^{n+1}$ velocity extrapolated to time-level $(n+1)$

What about tracers?

- A solution is to formulate the semi-implicit terms in flux-form

$$\overline{\rho\, q}_k^{n+1} = \left(\overline{\rho\, q}_k^{n+1}\right)_{exp} - \frac{\Delta t}{2}\left\{\nabla \cdot \left[\left(\overline{\rho\, q}_k^{n+1}\right)_{exp} \vec{v}_k^{n+1}\right] - \nabla \cdot \left[\left(\overline{\rho\, q}_k^{n}\right)_{exp} \tilde{\vec{v}}_k^{n+1}\right]\right\}.$$

so that reference states are eliminated (Wong et al., 2012)

Time-stepping and coupling: Eulerian flux-form

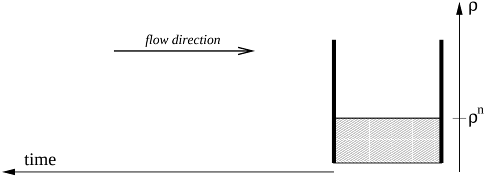

For efficiency, sub-cycle dynamics with respect to tracers:

- Solve continuity equation for air ρ together with momentum and thermodynamics equations.
- Repeat *ksplit* times
- Brown area = average flow of mass through cell face.
- Compute time-averaged value of q across brown area using flux-form scheme: $\overline{\overline{<q>}}$.
- Flux of tracer mass: $\overline{\overline{<q>}} \times \sum_{i=1}^{ksplit} \rho^{n+i/ksplit}$
- Yields 'free stream' preserving solution!

Time-stepping and coupling: Eulerian flux-form

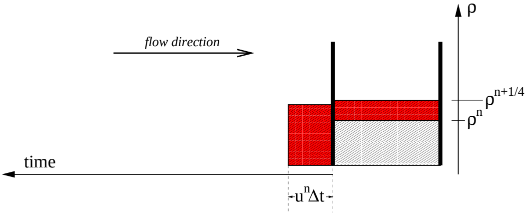

For efficiency, sub-cycle dynamics with respect to tracers:

- Solve continuity equation for air ρ together with momentum and thermodynamics equations.
- Repeat *ksplit* times
- Brown area = average flow of mass through cell face.
- Compute time-averaged value of q across brown area using flux-form scheme: $\overline{\overline{< q >}}$.
- Flux of tracer mass: $\overline{\overline{< q >}} \times \sum_{i=1}^{ksplit} \rho^{n+i/ksplit}$
- Yields 'free stream' preserving solution!

Time-stepping and coupling: Eulerian flux-form

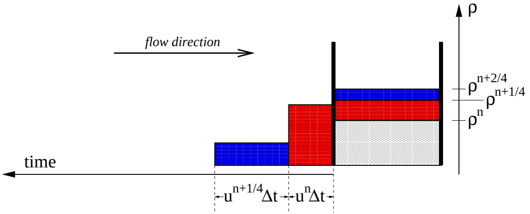

For efficiency, sub-cycle dynamics with respect to tracers:

- Solve continuity equation for air ρ together with momentum and thermodynamics equations.
- Repeat *ksplit* times
- Brown area = average flow of mass through cell face.
- Compute time-averaged value of q across brown area using flux-form scheme: $\overline{\overline{<q>}}$.
- Flux of tracer mass: $\overline{\overline{<q>}} \times \sum_{i=1}^{ksplit} \rho^{n+i/ksplit}$
- Yields 'free stream' preserving solution!

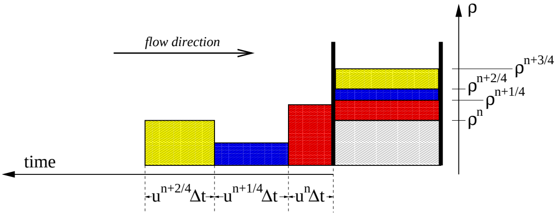

For efficiency, sub-cycle dynamics with respect to tracers:

- Solve continuity equation for air ρ together with momentum and thermodynamics equations.
- Repeat *ksplit* times
- Brown area $=$ average flow of mass through cell face.
- Compute time-averaged value of q across brown area using flux-form scheme: $\overline{\overline{<q>}}$.
- Flux of tracer mass: $\overline{\overline{<q>}} \times \sum_{i=1}^{ksplit} \rho^{n+i/ksplit}$
- Yields 'free stream' preserving solution!

Time-stepping and coupling: Eulerian flux-form

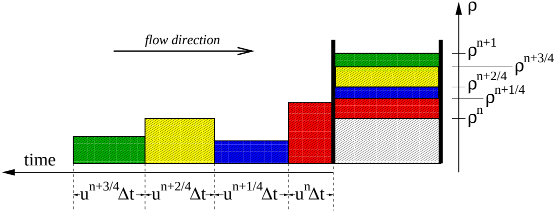

For efficiency, sub-cycle dynamics with respect to tracers:

- Solve continuity equation for air ρ together with momentum and thermodynamics equations.
- Repeat *ksplit* times
- Brown area = average flow of mass through cell face.
- Compute time-averaged value of q across brown area using flux-form scheme: $\overline{\overline{< q >}}$.
- Flux of tracer mass: $\overline{\overline{< q >}} \times \sum_{i=1}^{ksplit} \rho^{n+i/ksplit}$
- Yields 'free stream' preserving solution!

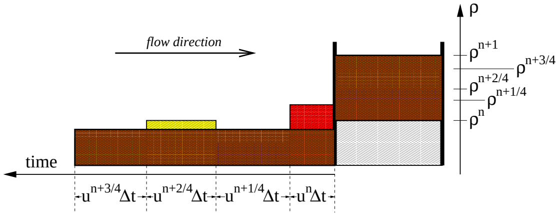

For efficiency, sub-cycle dynamics with respect to tracers:

- Solve continuity equation for air ρ together with momentum and thermodynamics equations.
- Repeat *ksplit* times
- Brown area = average flow of mass through cell face.
- Compute time-averaged value of q across brown area using flux-form scheme: $\overline{\overline{<q>}}$.
- Flux of tracer mass: $\overline{\overline{<q>}} \times \sum_{i=1}^{ksplit} \rho^{n+i/ksplit}$
- Yields 'free stream' preserving solution!

Questions?

References I

Barth, T. and Jespersen, D. (1989). The design and application of upwind schemes on unstructured meshes. *Proc. AIAA 27th Aerospace Sciences Meeting, Reno*.

Colella, P. and Woodward, P. R. (1984). The piecewise parabolic method (PPM) for gas-dynamical simulations. *J. Comput. Phys.*, 54:174–201.

Dukowicz, J. K. and Baumgardner, J. R. (2000). Incremental remapping as a transport/advection algorithm. *J. Comput. Phys.*, 160:318–335.

Durran, D. D. (1999). *Numerical Methods for Wave Equations in Geophysical Fluid Dynamics*. Springer-Verlag.

Harris, L. M., Lauritzen, P. H., and Mittal, R. (2010). A flux-form version of the conservative semi-Lagrangian multi-tracer transport scheme (CSLAM) on the cubed sphere grid. *J. Comput. Phys.*, 230(4):1215–1237.

Lauritzen, P. and Thuburn, J. (2012). Evaluating advection/transport schemes using interrelated tracers, scatter plots and numerical mixing diagnostics. *Quart. J. Roy. Met. Soc.*, 138(665):906–918.

Lauritzen, P. H., Erath, C., and Mittal, R. (2011a). On simplifying 'incremental remap'-type transport schemes. *J. Comput. Phys.*, 230:7957–7963.

Lauritzen, P. H., Kaas, E., Machenhauer, B., and Lindberg, K. (2008). A mass-conservative version of the semi-implicit semi-Lagrangian HIRLAM. *Q.J.R. Meteorol. Soc.*, 134.

Lauritzen, P. H., Nair, R. D., and Ullrich, P. A. (2010). A conservative semi-Lagrangian multi-tracer transport scheme (CSLAM) on the cubed-sphere grid. *J. Comput. Phys.*, 229:1401–1424.

Lauritzen, P. H., Skamarock, W. C., Prather, M. J., and Taylor, M. A. (2012). A standard test case suite for 2d linear transport on the sphere. *Geo. Geosci. Model Dev.*, 5:887–901.

Lauritzen, P. H., Ullrich, P. A., and Nair, R. D. (2011b). Atmospheric transport schemes: desirable properties and a semi-Lagrangian view on finite-volume discretizations, in: P.H. Lauritzen, R.D. Nair, C. Jablonowski, M. Taylor (Eds.), Numerical techniques for global atmospheric models. *Lecture Notes in Computational Science and Engineering, Springer, 2011*, 80.

Lin, S. J. and Rood, R. B. (1996). Multidimensional flux-form semi-Lagrangian transport schemes. *Mon. Wea. Rev.*, 124:2046–2070.

Machenhauer, B., Kaas, E., and Lauritzen, P. H. (2009). Finite volume methods in meteorology, in: R. Temam, J. Tribbia, P. Ciarlet (Eds.), Computational methods for the atmosphere and the oceans. *Handbook of Numerical Analysis*, 14. Elsevier, 2009, pp.3-120.

Margolin, L. G. and Shashkov, M. (2003). Second-order sign-preserving conservative interpolation (remapping) on general grids. *J. Comput. Phys.*, 184:266–298.

Miura, H. (2007). An upwind-biased conservative advection scheme for spherical hexagonal-pentagonal grids. *Mon. Wea. Rev.*, 135:4038–4044.

Nair, R. D. and Machenhauer, B. (2002). The mass-conservative cell-integrated semi-Lagrangian advection scheme on the sphere. *Mon. Wea. Rev.*, 130(3):649–667.

Nair, R. D., Scroggs, J. S., and Semazzi, F. H. M. (2002). Efficient conservative global transport schemes for climate and atmospheric chemistry models. *Mon. Wea. Rev.*, 130(8):2059–2073.

Ovtchinnikov, M. and Easter, R. C. (2009). Nonlinear advection algorithms applied to interrelated tracers: Errors and implications for modeling aerosol-cloud interactions. *Mon. Wea. Rev.*, 137:632–644.

Plumb, R. A. (2007). Tracer interrelationships in the stratosphere. *Rev. Geophys.*, 45(RG4005).

Rančić, M. (1992). Semi-Lagrangian piecewise biparabolic scheme for two-dimensional horizontal advection of a passive scalar. *Mon. Wea. Rev.*, 120:1394–1405.

Skamarock, W. C. and Menchaca, M. (2010). Conservative transport schemes for spherical geodesic grids: High-order reconstructions for forward-in-time schemes. *Mon. Wea. Rev.*, 138:4497–4508.

Thuburn, J. and McIntyre, M. (1997). Numerical advection schemes, cross-isentropic random walks, and correlations between chemical species. *J. Geophys. Res.*, 102(D6):6775–6797.

Trenberth, K. E. and Smith, L. (2005). The mass of the atmosphere: A constraint on global analyses. *J. Climate*, 18:864–875.

Ullrich, P., Lauritzen, P., and Jablonowski, C. (2012). Some considerations for high-order 'incremental remap'-based transport schemes: edges, reconstructions and area integration. *Int. J. Numer. Meth. Fluids*. revising.

Waugh, D. W., Plumb, R. A., Elkins, J. W., Fahey, D. W., Boering, K. A., Dutton, G. S., Volk, C. M., Keim, E., Gao, R.-S., Daube, B. C., Wofsy, S. C., Loewenstein, M., Podolske, J. R., Chan, K. R., Proffitt, M. H., Kelly, K. K., Newman, P. A., and Lait, L. R. (1997). Mixing of polar vortex air into middle latitudes as revealed by tracer-tracer scatterplots. *J. Geophys. Res.*, 120(D11):119–134.

Wong, M., Skamarock, W. C., and Lauritzen, P. H. (2012). A cell-integrated semi-implicit semi-Lagrangian shallow-water model (CSLAM-SW) with consistent treatment of inherently-conservative mass and scalar mass transport. *Mon. Wea. Rev.* in prep.

Zalesak, S. T. (1979). Fully multidimensional flux-corrected transport algorithms for fluids. *J. Comput. Phys.*, 31:335–362.

Zerroukat, M., Wood, N., and Staniforth, A. (2002). SLICE: A semi-Lagrangian inherently conserving and efficient scheme for transport problems. *Q. J. R. Meteorol. Soc.*, 128:2801–2820.

Zerroukat, M., Wood, N., and Staniforth, A. (2005). A monotonic and positive-definite filter for a semi-Lagrangian inherently conserving and efficient (SLICE) scheme. *Q. J. R. Meteorol. Soc.*, 131(611):2923–2936.